Weighted Relative Performance Ranking Function for Optimizing Reconfigurable Drones

Nitya Ravi*
University of California, Los Angeles, Los Angeles, CA, 90095

Neil Kaushikkar†
University of Illinois at Urbana-Champaign, Champaign, IL, 61820

Xander Zell‡
California Polytechnic State University, San Luis Obispo, CA, 93407

Felix Chen§
Worcester Polytechnic Institute, Worcester, MA, 01609

Julia Clark¶
University of California, Santa Barbara, Santa Barbara, CA, 93106

Alexandra Saccente‖
Oregon State University, Corvallis, OR, 97331

Gregor Limstrom**
Santa Clara University, Santa Clara, CA, 95053

Sierra Dabby††
Alhambra High School, Martinez, CA, 94553

Ryan Ehlmann‡‡
University of Houston, Houston, TX, 77004

Chloe Greenstein§§
Lewis & Clark College, Portland, OR, 97219

Bjorn Johnson¶¶
University of California, San Diego, La Jolla, CA, 92093

Michael Nguyen***
University of California, Irvine, Irvine, CA, 92697

Philip Quijano†††
University of California, Santa Cruz, Santa Cruz, CA, 95064

*Student, Astrophysics and Applied Mathematics
†Student, Computer Science
‡Student, Electrical Engineering
§Student, Computer Science and Robotics Engineering
¶Student, Physics
‖Student, Architectural Engineering
**Student, Computer Science and Engineering
††Student
‡‡Student, Supply Chain Logistics
§§Student, Physics
¶¶Student, Mechanical Engineering
***Student, Computer Engineering
†††Student, Electrical Engineering

Ajay Sunkara[‡‡‡]
Mountain View High School, Mountain View, CA, 94040

Annie Vu[§§§]
University of Texas at Dallas, Richardson, TX, 75080

Leonardo Bonanno[¶¶¶]
Stanford University, Stanford, CA, 94305

Nicholas Cramer[17]
NASA Ames Research Center, Moffett Field, CA, 94305

Parimal Kopardekar[18]
NASA Ames Research Center, Moffett Field, CA, 94305

Reconfigurable drones were developed, tested, and flown in multiple configurations in order to model flight characteristics for missions with varying requirements of employed drones. This resulted in the successful production of an evaluation function that identifies optimal drones for missions. Missions include tasks such as hovering in a desired position for a set amount of time, designated stationary flight, and flying a distance greater than one hundred meters and returning, designated long range flight. The ranking function considers a particular drone configuration's maximum payload, hover time, maximum speed, maximum range, and steadiness in relation to other drones and weighs each according to the requirements of the mission.

I. Nomenclature

A	=	effective area
B	=	battery capacity
C	=	battery C rating
C_D	=	drag coefficient
F_D	=	drag force
g	=	acceleration due to gravity
I	=	current
I_e	=	ESC rating
I_{hover}	=	current required to hover
I_m	=	motor continuous current rating
I_{pay}	=	current draw from payload
I_0	=	motor no-load current
k	=	motor thrust constant
k_t	=	torque-current proportionality constant
k_v	=	motor Kv
k_τ	=	torque thrust proportionality constant
k'	=	thrust-current proportionality constant
m_d	=	mass of drone
m_{pay}	=	mass of payload
n_m	=	number of motors
T	=	thrust

[‡‡‡]Student
[§§§]Student, Neuroscience
[¶¶¶]Student
[17]Technical Mentor
[18]Program Sponsor

T_{hover} = thrust required to hover
T_r = thrust ratio
t_{hover} = drone hover time
V_{nom} = battery nominal voltage
v = drone velocity
ρ = air density
τ = torque
ω = motor speed

II. Introduction

Unmanned aerial vehicles have a host of useful applications ranging from entertainment [1], to inspections [2], or package delivery.[3] Each of these applications have different flight domains. For a drone show precise localization and movement is paramount. On the other hand for power line inspection long duration flight is important but the payload size is less important than in the case for package delivery. While for normal business cases it makes sense to optimize the vehicle to the given use-case for cases where a few vehicles need to serve a variety of applications this presents a problem.

A potential solution is a reconfigurable drone. Reconfigurable drones are a cost-effective solution to this problem, as a single "kit" of modular drone components could theoretically allow a user to build hundreds of different drone variants, each with unique individual strengths. Much of the research on reconfigurable drones has been focused on the control of the vehicle in all the configurations.[4] That is critical work but it does not address the need for the operator to easily down select the potential reconfigurations to their application.

To solve this issue, we designed a ranking function that incorporates what we consider to be the five different characteristics of a drone configuration: maximum payload capacity (based on the drone's ability to take off), maximum hover time, maximum speed, maximum range, and the drone's steadiness based on its moment of inertia. This ranking system considers all combinations of drone parts from a given set of parts, filters out impractical drones, and weighs the performance of these characteristics based on a task or mission chosen by the user before returning the best subset of drones for the specific mission.

III. Modeling

In order to create a ranking function that produces the optimal drone, the different characteristics of a drone must first be modeled. The characteristics that we considered in our ranking function are maximum payload, hover time, moment of inertia, range, and top speed. These are modeled below, and the modeling process can be seen in Figure 22.

A. Takeoff

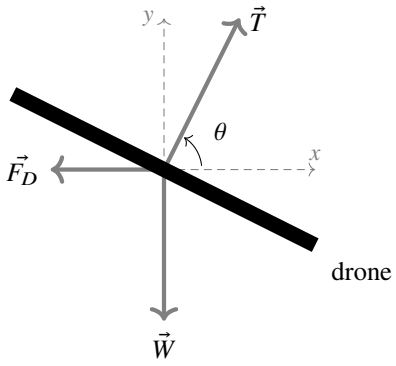

Fig. 1 Drone Force Diagram

For calculations, we used the assumption that a drone can take off if it can achieve a 2:1 thrust to weight ratio. Since the drone takes off from standing on its legs, the thrust in Figure 1 $\vec{T}$ is vertical and θ is 90 degrees. That is, it can produce thrust at least equal to twice its weight including the payload. This ratio is greater than 1:1 in order to account for inconsistency between parts like the motors and ESCs as seen in Figure 2, and to maintain altitude while changing directions because the design of the drones we used dictates that not all motors provide their full force at all times, especially while moving quickly.

$$T_{max} \geq 2\,(m_d + m_{pay})\,g \tag{1}$$

Torque and thrust are approximately proportional, and torque is approximately proportional to the current minus the no-load current [5].

$$k_\tau = \frac{\tau}{T} \tag{2}$$

$$\tau = k_t(I - I_0) \tag{3}$$

k_t is the torque-current proportionality constant. This value is specific to a motor and can be determined from the motor Kv using the following equation [5].

$$k_t = \frac{60}{2\pi k_v} \tag{4}$$

Thrust and current can then be related by k' as follows. k' is calculated using dynamometer tests across three motors for each motor and propeller combination. The k' values for compatible motor-propeller combinations are listed in Figure 23.

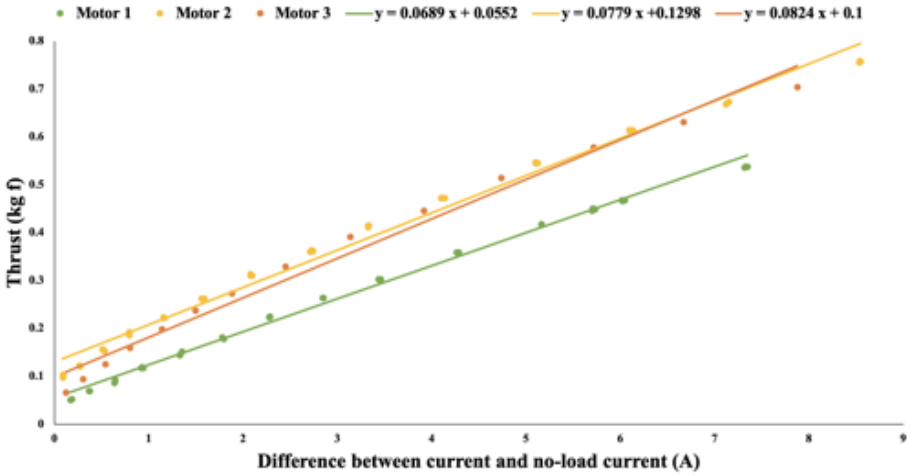

Fig. 2 k' constant inconsistency of motors

$$k' = \frac{k_t}{k_\tau} \tag{5}$$

$$T = k'(I - I_0) \tag{6}$$

The maximum thrust produced by the drone as limited by the maximum current is as follows.

$$T_{1max} = k'(I_{max} - I_0)n_m \tag{7}$$

Where I_{max} is the maximum current as limited by the motors, ESCs, batteries, and payload, and n_m is the number of motors.

The three limiting factors for the current are the motor max continuous current I_m, the ESC amp rating I_e, and the battery output as follows

$$I_b = \frac{BC - I_{pay}}{n_m} \tag{8}$$

Then the maximum current is

$$I_{max} = min(I_m, I_e, I_b) \tag{9}$$

The thrust is not just limited by the current, but it is also limited by the maximum speed of the motors.

$$\omega_{max} = k_v V_{nom} \tag{10}$$

The thrust is approximately proportional to the square of the motor speed [5]. So the maximum thrust based on motor speed is

$$T_{2max} = k\omega_{max}^2 n_m \tag{11}$$

k is calculated through dynamometer tests of different motor and propeller combinations. The k values for compatible motor-propeller combinations are listed in Figure 24. The maximum thrust that the drone can produce is

$$T_{max} = min(T_{1max}, T_{2max}) \tag{12}$$

If this value T_{max} is greater than or equal to twice the weight of the drone and its payload, then the drone can take off.

Since a drone must be able to take off in order to complete a flight, the maximum mass of the payload is

$$m_{pay} \leq \frac{T_{max}}{2g} - m \tag{13}$$

B. Hover Time

The hover time t_{hover} is based on how long the battery can maintain the current I_{hover} required to hover.

$$t_{hover} = \frac{B}{n_m I_{hover} + I_{pay}} \tag{14}$$

In order for the drone to hover, the thrust must be equal to the weight of the drone and its payload.

$$T_{hover} = (m_d + m_{pay})g \tag{15}$$

$$T_{hover} = n_m k'(I_{hover} - I_0) \tag{16}$$

So the current required to hover is shown in the equation below.

$$I_{hover} = \frac{(m_d + m_{pay})g}{n_m k'} - I_0 \tag{17}$$

C. Top Speed

The drone moves at a constant velocity when the thrust in the direction of motion is equal to the drag force which always opposes the direction of the drone's velocity. In Figure 1, the drone's velocity is in the positive x direction and the drag force acts in the negative x direction. From Figure 1 we can ascertain that

$$Tsin\theta = g(m_d + m_{pay}) \tag{18}$$

$$T = |\vec{T}| \tag{19}$$

We define the thrust ratio as

$$T_r = \frac{T}{(m_d + m_{pay})g} \tag{20}$$

$$sin\theta = \frac{1}{T_r} \tag{21}$$

The drag force on the drone is as follows [5]

$$F_D = \frac{1}{2}\rho C_D A v^2 \tag{22}$$

where C_D is the drag constant, A is the effective area of the surface in the direction of motion, and ρ is the air density. Because the modeling of the drones is for the purpose of ranking them, C_D need not be altered for different drone configurations.

The drone moves at a constant velocity when drag and thrust are equal.

$$F_D = Tcos\theta \tag{23}$$

$$\frac{1}{2}\rho C_D A v^2 = T_r(m_d + m_{pay})g\sqrt{1 - \frac{1}{T_r^2}} \tag{24}$$

The velocity can be written as follows

$$v = \sqrt{\frac{2T_r(m_d + m_{pay})g}{\rho C_D A}}(1 - \frac{1}{T_r^2})^{1/4} \tag{25}$$

The maximum speed is when this term is maximized.

D. Range

From equations 6 and 20, we get

$$T_r(m_d + m_{pay})g = k'(I_v - n_m I_0) \tag{26}$$

where I_v is the current required for the drone to fly at velocity v from equation 25.

$$I_v = \frac{T_r(m_d + m_{pay})g}{k'} - n_m I_0 \tag{27}$$

The time that the battery can sustain this current is

$$t_{range} = \frac{B}{I_v + I_{pay}} \tag{28}$$

Thus, the range of the drone is

$$R = v t_{range} \tag{29}$$

E. Steadiness

We can define the steadiness of a drone by the amount of force needed to change its current state of momentum, commonly defined as inertia. The greater the drone's moment of inertia, the steadier the drone. Since we are using the moment of inertia for ranking, we chose to approximate the measurements because they do not need to be exact, just demonstrate relative design differences in a quantifiable manner. The different drone parts can be approximated as regular shaped solids and point masses as long as the approximations are consistent across the different drone configurations. The frame of the drone is approximated as a rectangular prism as seen in Figure 3. The axis of rotation passes through the center of one face of the frame such that it is at a right angle to the face. As seen in Figure 5, this is so that the batteries are not on the axis and are accounted for in the moment of inertia calculation. The arms of the drone are approximated as rods with uniform mass density as seen in Figure 4. The motors, propellers, ESCs, and batteries are all considered to be point masses. Their sizes can be considered negligible because they are small compared to the frame and the arms. The landing gear of the drone is not incorporated into the moment of inertia calculation because

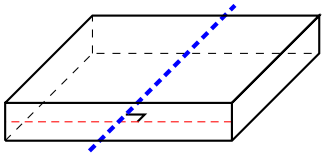

Fig. 3 Drone Frame Approximation

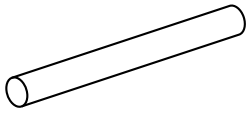

Fig. 4 Drone Arm Approximation

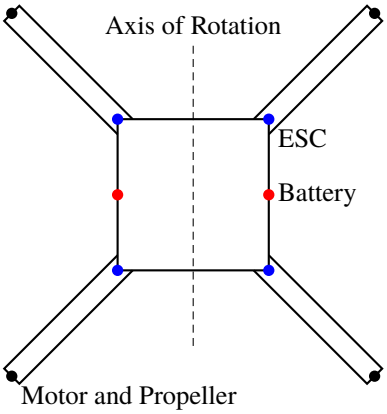

Fig. 5 Quadcopter Approximation

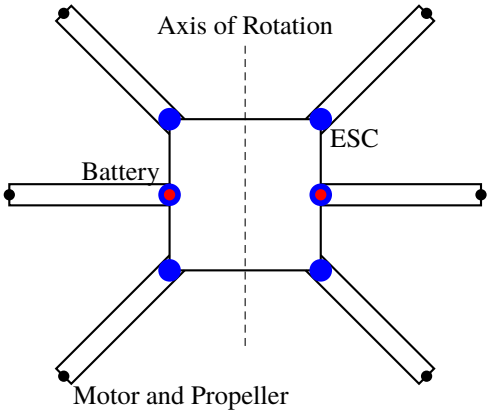

Fig. 6 Hexacopter Approximation

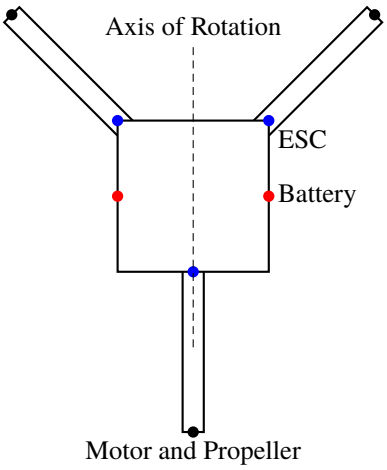

Fig. 7 Tricopter Approximation

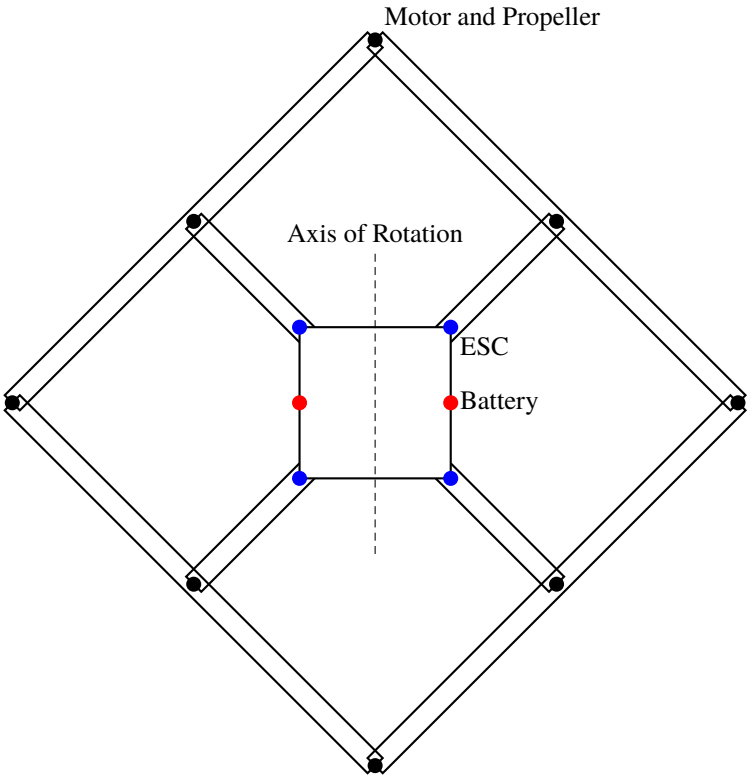

Fig. 8 Gridcopter Approximation

the purpose of these calculations is for ranking and the legs are uniform across each configuration. Figures 5, 6, 7, and 8 show the top down view of the approximation of four different configurations.

These models are used to find how well drone configurations perform in terms of each characteristic compared to one another. We defined four different missions – high speed flight, long range flight, stationary flight, and precision flight. For each mission, characteristics are weighted differently based on which are more important for the given task. The models were confirmed and refined through flight testing of different drone configurations performing different missions.

IV. Test Setup

A. Indoor Flight Tests

All test flights to confirm vehicle performance took place inside the NASA small Unmanned aerial systems Autonomy Research Complex (NUARC) at Ames Research Center. Within the building, there is a large netted cage for flying most missions, and a region outside the cage for unrestricted flight. All preliminary setup of drones takes place in the netted part of the facility. The following tests also take place in the net: Hover, Payload Capacity, and Tuning. Distance and Speed testing take place in the unrestricted flight region of the NUARC facility. Tests were performed in order to determine the accuracy of the model of the drone used. Unfortunately, only the maximum hover time and maximum payload equations could be tested properly as the indoor facility made it impossible to test the top speed of the drone and the true maximum range of the drone, as presumably in practice the drone would not be repeatedly speeding up and slowing down during flight. Precision is intended to be tested by filming video recorded on different drones and having users rank the shakiness of the drone, but this metric is not precise since no quantitative values can be obtained from performing these sorts of tests. Future work will involve more extensive testing and equation verification. Additionally, as only the three drone configurations in Figures 11, 12, and 13 have been tested so far, future work involving testing of many types of drones will prove valuable to see how the drones compare in practice and if our downselection process

performs this ranking well.

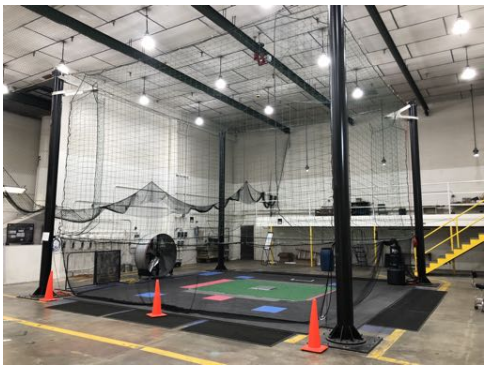

Fig. 9 The netted testing area

Fig. 10 The unrestricted flight area

Fig. 11 Gridcopter

Fig. 12 Quadcopter

Fig. 13 Tricopter

Testing in the NUARC facility eliminates weather concerns and reduces possibilities for unsafe conditions. However, it precludes the usage of GPS, making autonomous flight difficult without an additional localization system.

In order to confirm that the equations we use for our modeling and ranking are correct, we run flight tests in four patterns: Hover, Payload, Traversal, and Tuning.

1) Hover: To measure the vehicle's hovering capabilities, we fly the UAV directly above a camera on the floor, and hover in place there, using only as much throttle/control input as is necessary to maintain position. Once there, we measure the time until the vehicle reaches low battery. The results of this test are compared against the hover time calculations from section III.B. Additionally, we compare the videos taken of the vehicles hovering against the videos from other vehicles, which we use to rank the relative stability of each vehicle in a constant position.
2) Payload: We attach boxes of ballast to the underside of the vehicle, and increase the mass until it is no longer capable of flight. It is important to note that due to aerodynamics near the ground and voltage drop due to internal resistance, vehicles at the maximum limit may briefly jump into the air but be unable to maneuver or maintain altitude. For accuracy, we only count a flight as successful if it can maintain an altitude of 2 meters for 30 seconds. As with hover time, we compare the result of this test against the maximum payload calculation in section III.A.
3) Range: Within the unrestricted region of the NUARC building, we mark out a straight line and measure the length of said line. The pilot then flies the UAV from endpoint to endpoint until the vehicle is at low battery. The vehicle does not land in the middle of the test. Adding up the total number of trips and multiplying that by the length of the line yields the maximum range. This test also measures the velocity on each leg of the path, by measuring the time for one line, and the average velocity for the whole trip.
   Due to space limitations inside NUARC, the path for the vehicle in our tests is 16.03 meters. This will cause our test to underestimate the distance a vehicle can travel because it will include the extra power draw of stopping the vehicle more frequently.

4) Tuning: A vehicle's tuning is a subjective measurement, defined by how the pilot feels when controlling the vehicle. To test the tuning, the pilot hovers the vehicle and makes rapid movements with the control sticks. A well-tuned vehicle will feel stable and responsive, while a poorly-tuned vehicle may feel sluggish, unstable, or over-corrective; the pilot is responsible for communicating what they feel when controlling the vehicle.

B. Dynamometer Tests

Information describing the performance of our motors and propellers is important in making correct predictions about UAV capabilities. The most important value of dynamometer testing yields is k'. To measure the motors included in the project, we use an RCBenchmark series 1580 Thrust Stand and Dynamometer, along with a SkyRC 1200W/50A Power Supply. Additionally, a computer is necessary to run the RCBenchmark software and to save test logs.

For each motor that we want to test, we attach a propeller and then run the motor at its minimum throttle. At this point, we take three measurements, before increasing the motor speed in 250 RPM increments. After each increment, we log three more measurements. We continue increasing RPM until the hardware hits one of the safety limits. For safety, and to avoid burning out motors, we let the motor cool off completely before putting on the next propeller. Additionally, some motor-propeller combinations (specifically high kV motors with short propellers) can reach RPMs where it is no longer feasible to perform 250 RPM increments, as running the dynamometer at high current for too long can damage the motor. If this is the case, it is recommended to raise the increment to 500 or 1000 RPM steps.

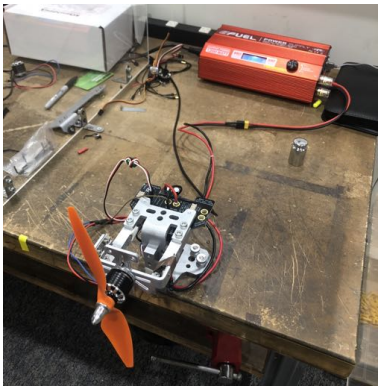

Fig. 14 Dynamometer Setup

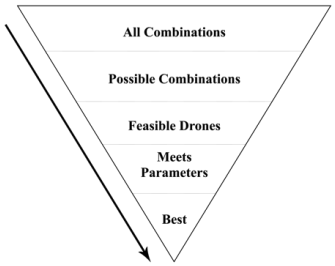

Fig. 15 Downselection Process

V. Methodology

The different mechanical and electrical components of the drone can be reconfigured to change the values for the flight characteristics detailed in the modeling section. These include the frame configuration, batteries, propellers, motors, and electronic speed controllers (ESC). Certain combinations of these different parts produce optimal drones for specific missions and user input requirements. An example list of parts can be found in Figure 25 and the changeable electrical components can be seen in Figure 26.

The process to select the best drone for a selected mission begins with a filtering process to reduce all possible combinations of parts down to a handful of drones. We begin the downselection process by eliminating combinations that are impossible to build. These include incompatible propellers and motors and incompatible propellers in drone configurations. Some propellers are too long for certain drone configurations as the propellers collide when rotating. Next, we eliminate all drones unable to meet a minimum of a 2:1 thrust to weight ratio. Payloads that the drones are carrying are included in the weight of the drone when determining the ratio. Next, all drones that do not meet the user-defined parameters of minimum flight time, minimum payload capacity, and minimum range are filtered out. Finally, we apply our ranking function to determine the handful of optimal drone configurations and electronic parts that satisfy the mission parameters.

Our ranking formula weights each of 5 performance categories (Equation 30) before summing each weighted rank to obtain the final rank. The weights of each characteristic range from 0 to 5 and are dependent on the mission selected. Weights are defined by users after selecting mission types. Our ranking function begins by normalizing flight characteristics—payload capacity, hover time, the moment of inertia, flight range, and max flight velocity—for all drones available to a user (Equation 32). Then, the function determines whether to penalize drones lacking in any category. The function assigns a multiplier penalty of -2.5 for each characteristic in all drones with normalized flight characteristics less than the defined limit (Equation 31). We decided to penalize drones lacking in categories prioritized by users, so subpar categories important to a selected mission are not compensated for by superior flight characteristics

unrelated to the chosen mission. We also decided that 2.5 high category performances are sufficient to compensate for one subpar category performance. We chose the limit values in order to simply consider the top few drones of each category. The score for each category (Equation 34) is determined by multiplying the user-defined category weight, the category penalty, and the square of the difference between the normalized category value and the category limits. We square the difference in category value and category limits to exaggerate the difference and further separate drones with subpar flight characteristics from those with superior category performances. The positions (1, 1) through (5, 5) in all of the following matrices correspond to flight time, hover time, the moment of inertia, flight range, and max flight velocity, respectively. The final drone rank is obtained by summing the 5 category scores (Equation 35). Higher ranks correspond to drones with better overall performances based on the user-defined weights corresponding to the chosen mission categories.

$$weights = \begin{bmatrix} W_1 & 0 & \cdots & & 0 \\ \vdots & W_2 & & & \\ & & W_3 & & \vdots \\ & & & W_4 & 0 \\ 0 & & \cdots & 0 & W_5 \end{bmatrix} \tag{30}$$

$$penalty = \begin{bmatrix} -2.5 \text{ or } 1 & 0 & \cdots & & 0 \\ \vdots & -2.5 \text{ or } 1 & & & \\ & & -2.5 \text{ or } 1 & & \vdots \\ & & & -2.5 \text{ or } 1 & 0 \\ 0 & & \cdots & 0 & -2.5 \text{ or } 1 \end{bmatrix} \tag{31}$$

$$norm = \begin{bmatrix} 0 \to 1 & 0 & \cdots & & 0 \\ \vdots & 0 \to 1 & & & \\ & & 0 \to 1 & & \vdots \\ & & & 0 \to 1 & 0 \\ 0 & & \cdots & 0 & 0 \to 1 \end{bmatrix} \tag{32}$$

$$limits = \begin{bmatrix} 0.8 & 0 & \cdots & & 0 \\ 0 & 0.8 & & & \vdots \\ \vdots & & 0.7 & & \\ & & & 0.7 & 0 \\ 0 & \cdots & & 0 & 0.7 \end{bmatrix} \tag{33}$$

$$category\ score = penalty * weight * (norm - limit)^2 \tag{34}$$

$$rank = trace(category\ score) \tag{35}$$

VI. Results

To validate our ranking function, we explored two test missions with two drones each. The first mission was a stationary flight mission with a desired hover time of two minutes and a payload of 0.2 kg. The two characteristics important to this mission are hover time and steadiness. As shown in Figure 16, a gridcopter should be more suited for this mission than a quadcopter because it has greater steadiness. However, both can reach the minimum desired hover time and can be used for the mission.

Figure 18 and 19 show that the gridcopter was able to hover in the desired position better than the quadcopter. The gridcopter was able to maintain this position within a 0.3 meter by 0.3 meter square whereas the quadcopter could not hover within this range and moved up to 1.2 meters away from the desired position. This confirms the information in Figure 16.

The second mission was a long range test with a desired distance of 300 meters and a payload of 0.1 kg. Figure 17 shows that the quadcopter is better than a gridcopter for a long range mission since the quadcopter is optimized for range and flight time, the necessary flight characteristics for this mission. This flight test was conducted by flying the drone back and forth over laps of 6.807 meters. Figure 17 highlights the fact that despite the fact that the lowest ranking drone performed better than the best 2 drones of different arm configurations in 2 separate categories, the lowest ranking drone did not perform well in categories deemed important to the long-range flight mission. Therefore, the ranking function assigned it the lowest score.

Figure 16 highlights the fact that a drone with mediocre flight characteristics can compensate with other strengths. The gridcopter at rank 1 has an average flight time but makes up for that with high maximum payload capacity. The high hover-mission-critical steadiness accompanied by the high maximum payload and average performances in the remaining categories leads the gridcopter to rank 1. However, the ranking function has a slight shortcoming. The hovering mission deems steadiness and flight time important. In this selection, the ranking function leaves the best choice slightly ambiguous. There is no drone with standout performances in these two important categories. The function leaves the user with a choice between a gridcopter with high stability and high maximum flight capacity and the rank 2 quadcopter with high flight time and high flight range. The user would require some drone piloting experience to choose the absolute best drone for a specific situation. The best way to fix the issue is to allow users to elaborate on the mission parameters, but we ultimately against extremely detailed mission definitions to hasten the user-experience and abstract the ranking process to help less experienced pilots.

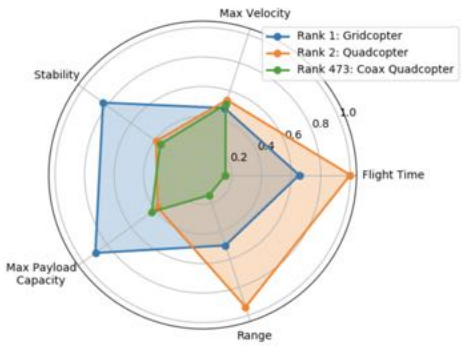

Fig. 16 Stationary Flight Characteristics

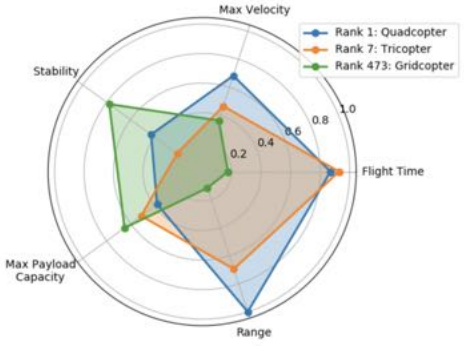

Fig. 17 Range Flight Characteristics

Figure 20 shows that the grid was not able to complete the mission and flew less than half the desired range. Figure 19 shows that the quadcopter successfully completed the mission. This validates the ranking of the quadcopter as better than the gridcopter for long range flight.

The long range flight tests were conducted in an enclosed space. Ideally, the test area would allow the drone to fly 300 meters in a single direction. Because of this limitation, energy was lost each time the drone turned at the end of a lap. This greatly affected the gridcopter's inability to complete the mission. Both the gridcopter's greater mass and it's higher stability made it difficult for the drone to perform quick and efficient turns, so the gridcopter lost a higher amount of energy on each turn. However, the quadcopter still performed better than the gridcopter, fulfilling the expectations set by the ranking function.

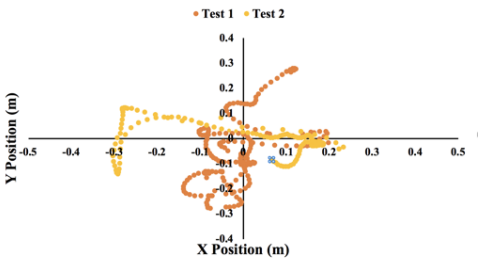

Fig. 18 Gridcopter Stationary Flight Test

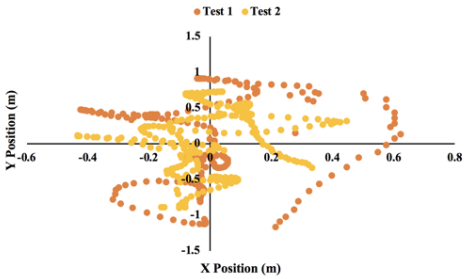

Fig. 19 Quadcopter Stationary Flight Test

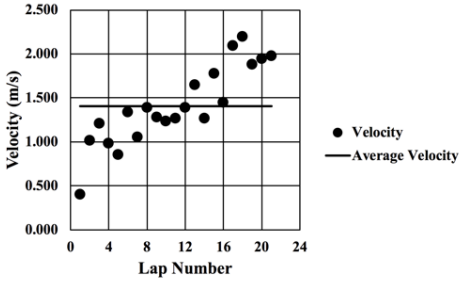

Fig. 20 Gridcopter Range Test

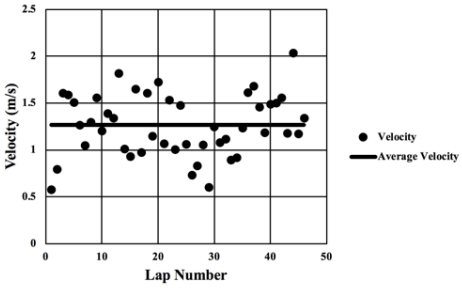

Fig. 21 Quadcopter Range Test

Appendix

Modeling Process

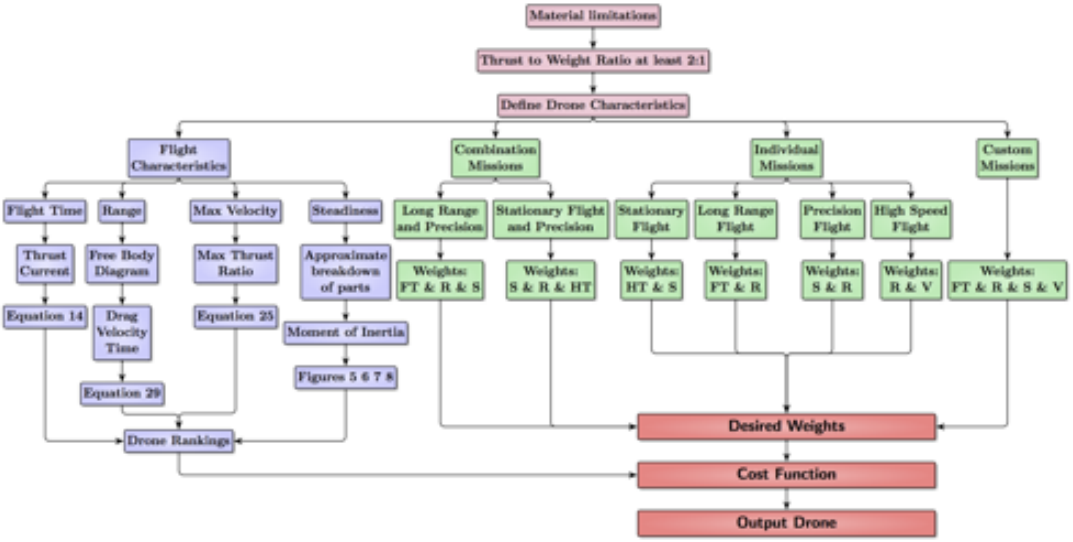

Fig. 22 Modeling Process

k and k' Values

The following charts show the k and k' values calculated for compatible motor-propeller combinations. The hyphens indicate incompatible combinations. The values were calculated from data collected through dynamometer tests.

	470 Kv Motor	**965Kv Motor**	**2050Kv Motor**
18 in. Prop	0.98073788	-	-
16 in. Prop	1.055890551	-	-
14 in. Prop	1.023636027	-	-
11 in. Prop	1.055757168	0.781490722	-
10 in. Prop	1.147421197	0.750462143	-
9 in. Prop	1.222554163	0.756210847	-
8x4.5 in. Prop	-	-	0.424823103
8x3.8 in. Prop	-	0.707182503	0.549960576
6 in. Prop	1.05265541	0.700712379	0.506781437

Fig. 23 k' Values

	470Kv Motor	**965Kv Motor**	**2050Kv Motor**
18 in. Prop	0.0000731495	-	-
16 in. Prop	0.000051226	-	-
14 in. Prop	0.0000365903	-	-
11 in. Prop	0.000018211	0.0000246594	-
10 in. Prop	0.0000185391	0.0000140134	-
9 in. Prop	0.0000183236	0.00000980179	-
8x4.5 in. Prop	-	-	0.0000062226
8x3.8 in. Prop	-	0.00000747808	0.00000750747
6 in. Prop	0.00001834409	0.00000202781	0.00000210191

Fig. 24 k Values

Drone Parts

The following figure shows a sample list of changeable drone parts. These parts can be combined in many different ways to produce a variety of drone configurations.

Arm Configurations	6	Tricopter (With SERVO motor) Quadcopter Coaxial Quadcopter Hexacopter 6-motor H formation 8-motor Grid									
Batteries	4	Capacity (mAh)		C Rating		Mass (g)		# of Cells			
		2700		35		265.5		4SIP			
		2500		30		194.3		3SIP			
		1800		75		202.1		4SIP			
		850		75		97.4		4SIP			
Propellers	9	Diameter (in)		Pitch (in/rot)		Mass (g)					
		11		4.7		14.1					
		10		4.5		11.2					
		9		4.5		7.1					
		6		4		6.9					
		8		3.8		7					
		8		4.5		7.1					
		16		5.5		61.7					
		18		5.5		61.7					
		14		4.7		25.2					
Motors	3	Mass (kg)	Motor No Load Current	kV of Motor (RPM/V)		Kt of Motor (N*m/A)		Max Continuous Current (A)		Motor Radius	
		0.1187	0.3	470		0.02031765		15		0.02	
		0.0961	0.5	965		0.009895644		26		0.015	
		0.946	1.3	2050		0.004658193		44		0.015	
ESC	3	Name		Mass (g)		Continuous Current (A)		Pixhawk Compatibility			
		KDEXF-UAS20LV		29.6		20		With Modification			
		KDEXF-UAS35		52.7		35		With Modification			
		Turnigy Plush-60		70.8		60		Yes			

Fig. 25 Sample Drone Parts List

The following diagram shows how different electrical parts can be exchanged to produce drone's with different capabilities.

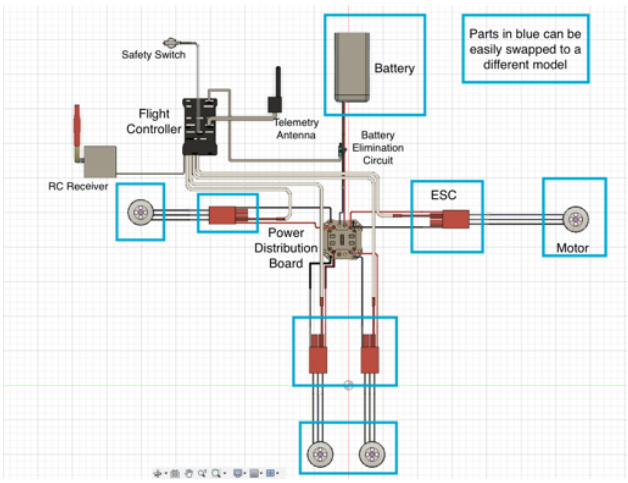

Fig. 26 Changeable Electrical Components

Additional Flight Characteristic Comparisons

The following diagrams show how drone configurations compare when flight time, steadiness, and speed are prioritized.

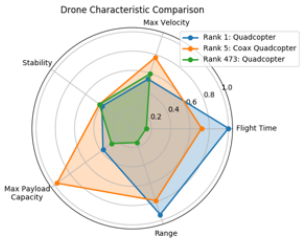

Fig. 27 Flight Time

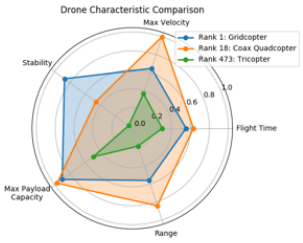

Fig. 28 Steadiness

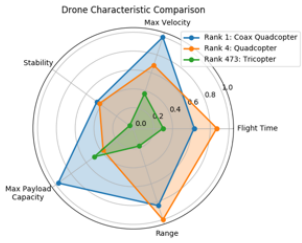

Fig. 29 Speed

Mission Definitions

Stationary Flight: The drone is able to take off, travel a maximum distance of 100 meters away from the starting point, fly in place at the destination, and return to the starting point with a maximum round trip distance of 200 meters. This mission is ideal for surveying areas.

Precision Flight: This mission is ideal for flying in constrained spaces during flight or if a fragile payload is present.

Long Range: The drone is able to travel between 200 meters and 6 kilometers total as desired by the user.

High Speed: This mission is ideal for fast flight, including racing and delivering perishables.

Acknowledgments

This research was supported by NASA Ames Research Center, by providing the project funding, materials and technology resources, and the testing facility. In addition, this research was supported by the Universities Space Research Association for also funding the project. The authors would like to thank their technical mentors, Nicholas Cramer and David Murakami, who provided insight and expertise that greatly assisted the research. The authors are immensely grateful to Evan Kawamura for his constant knowledge and support. They would especially like to thank their project sponsor, Parimal Kopardekar, for their time and support. Lastly, they thank Bimal Aponso, Jeff McCandless, and Corey Ippolito for making this project possible.

References

[1] Waibel, M., Keays, B., and Augugliaro, F., "Drone shows: Creative potential and best practices," Tech. rep., ETH Zurich, 2017.

[2] Jones, D., "Power line inspection-a UAV concept," *2005 The IEE Forum on Autonomous Systems (Ref. No. 2005/11271)*, IET, 2005, pp. 8–pp.

[3] Singireddy, S. R. R., and Daim, T. U., "Technology Roadmap: Drone Delivery–Amazon Prime Air," *Infrastructure and Technology Management*, Springer, 2018, pp. 387–412.

[4] Niemiec, R., Gandhi, F., and Singh, R., "Control and performance of a reconfigurable multicopter," *Journal of Aircraft*, Vol. 55, No. 5, 2018, pp. 1855–1866.

[5] Gibiansky, A., "Quadcopter Dynamics, Simulation, and Control," 2012. URL http://andrew.gibiansky.com/downloads/pdf/Quadcopter%20Dynamics,%20Simulation,%20and%20Control.pdf